Available online at www.sciencedirect.com
SCIENCE DIRECT®
Biochemical Pharmacology 68 (2004) 689–698
Biochemical Pharmacology
www.elsevier.com/locate/biochempharm

Peripheral-type benzodiazepine receptor density and in vitro tumorigenicity of glioma cell lines

Leo Veenman[a,1], Evgeny Levin[a,1], Gary Weisinger[b], Svetlana Leschiner[a], Ilana Spanier[a], Solomon H. Snyder[c], Abraham Weizman[d], Moshe Gavish[a,*]

[a]*Department of Pharmacology, Rappaport Family Institute for Research in the Medical Sciences, Technion-Israel Institute of Technology, P.O.B. 9649, Bat-Galim, Haifa 31096, Israel*
[b]*Tel Aviv Sourasky Medical Center, The Endocrine Institute, Tel Aviv, Israel*
[c]*Department of Neuroscience, Pharmacology and Molecular Sciences and Psychiatry, School of Medicine, The Johns Hopkins University, Baltimore, MD, USA*
[d]*Geha Mental Health Center, Felsenstein Medical Research Center, Rabin Medical Center, Sackler Faculty of Medicine, Beilinson Campus, Tel Aviv University, Petah Tiqva, Israel*

Received 11 January 2004; accepted 4 May 2004

Abstract

The peripheral-type benzodiazepine receptor is found primarily on the outer mitochondrial membrane and consists of three subunits: the 18 kDa isoquinoline binding protein, the 32 kDa voltage-dependent anion channel, and the 30 kDa adenine nucleotide transporter. The current study evaluates the potential importance of peripheral-type benzodiazepine receptor expression in glioma cell tumorigenicity. While previous studies have suggested that peripheral-type benzodiazepine receptor-binding may be relatively increased in tumor tissue and cells, so far, little is known about the relationships between peripheral-type benzodiazepine receptor density and factors underlying tumorigenicity. In the present study, we found in glioma cell lines (C6, U87MG, and T98G), that peripheral-type benzodiazepine receptor ligand-binding density is relatively high for C6 and low for T98G, while U87MG displays intermediate levels. Cell growth of these cell lines in soft agar indicated that high levels of peripheral-type benzodiazepine receptor-binding were associated with increased colony size, indicative of their ability to establish anchorage independent cell proliferation. Potential causes for differences in tumorigenicity between these cell lines were suggested by various cell death and proliferation assays. Cell death, including apoptosis, appeared to be low in C6, and high in T98G, while U87MG displayed intermediate levels in this respect. Cell proliferation appeared to be high in C6, low in T98G, and intermediate in U87MG. In conclusion, our study suggests that relatively high peripheral-type benzodiazepine receptor-binding density is associated with enhanced tumorigenicity and cell proliferation rate. In particular, apoptosis appears to be an important tumorigenic determinant in these glioma cell lines. Moreover, application of PBR-specific ligands indicated that PBR indeed are functionally involved in apoptosis in glioma cells.

Keywords: Glioma; Peripheral-type benzodiazepine receptor; Ligand-binding; Tumorigenicity; Soft agar; Proliferation; Apoptosis

Peripheral-type benzodiazepine receptor(s) are abundant in peripheral tissues [1,2] as well as in glial cells of the CNS [3–5], and are located primarily on mitochondrial membranes [6–9]. Functional PBR are constituted of at least three protein components (see Fig. 1): (i) the 18 kDa isoquinoline-binding protein (IBP); (ii) the 32 kDa voltage-dependent anion channel (VDAC); and (iii) the 30 kDa adenine nucleotide transporter (ANT) [10]. Specific PBR ligands include the benzodiazepine Ro5-4864 (4′-chlorodiazepam), the isoquinoline carboxamide derivative, PK 11195, and FGIN-1-27 (*N*,*N*-di-*n*-hexyl 2-(4-fluorophenyl)indole-3-acetamide) [11–13]. Topographic analysis of the receptor distribution on the mitochondrial membrane has indicated that the receptor complex is formed by several 18 kDa subunits associated

Abbreviations: ABTS, 2,2′-azino-bis-[3-ethylbenzothiazoline]-6-sulfonic acid; ANT, adenine nucleotide transporter; FACS, fluorescence-assisted cell sorting; IBP, isoquinoline-binding protein; PBR, peripheral-type benzodiazepine receptor(s); PBS, phosphate buffered saline; PMSF, phenylmethylsulfonyl fluoride; SDS, sodium dodecyl sulfate; VDAC, voltage-dependent anion channel

* Corresponding author. Tel.: +972 4 8295275; fax: +972 4 8295271.
E-mail address: mgavish@tx.technion.ac.il (M. Gavish).
[1] Equal contribution to this study.

0006-2952/$ – see front matter © 2004 Elsevier Inc. All rights reserved.
doi:10.1016/j.bcp.2004.05.011

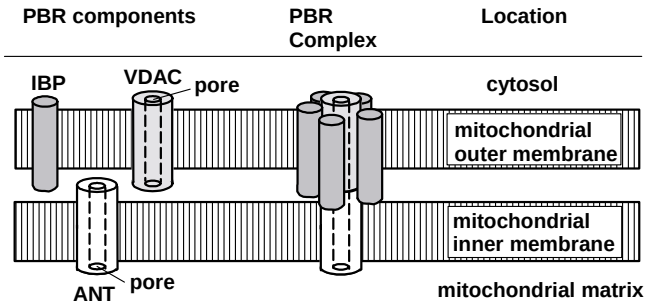

Fig. 1. Location of the PBR complex and its protein components in the mitochondrial membrane.

with one VDAC molecule and that this complex is located on the outer- and inner-mitochondrial membrane contact sites [14]. In addition, it appears that the ratio of IBP to VDAC and ANT is tissue- and condition-specific [15,16]. Structurally, VDAC forms the core of the receptor complex, which in addition to IBP and ANT, may include proteins of the Bcl-2 family and creatine kinase [17–19].

Peripheral-type benzodiazepine receptor(s) have been implicated in various functions: mitochondrial steroid production [20–24], mitochondrial respiration [25,26], modulation of voltage-dependent calcium channels [27], immune and phagocytic host defense response [28,29], cell growth and differentiation [30–32], responses to stress [33,34], inflammation [35], microglial activation related to brain damage [16,36–38], and tumor proliferation [24,32,39], including glial tumors [40,41].

Using mouse thymoma cells, Wang et al. [30] were the first to show a strong and positive correlation between the anti-proliferative activity and the affinity of phosphate buffered saline (PBR) ligands. We and others found that PBR levels are increased in tumorigenic tissues, for review, see Gavish et al. [39]. A recent study, using stage III colorectal cancer tissue, suggests that over-expression of PBR can serve as a prognostic marker [42]. In addition, specific PBR ligands were found to induce apoptosis and cell cycle arrest in human colorectal cancer cells [43]. These findings suggest that PBR are involved in growth control as well as cellular proliferation of carcinogenic tissue, and that apoptosis may form one of the mechanisms for this involvement.

Several studies have demonstrated an increased binding of PBR ligands in different brain tumors [44–46]. This property can be used to accurately delineate glioma borders using positron emission tomography [47]. For example, in rat C6 glioma PBR densities are increased up to 30-fold compared to surrounding neocortex [46,48]. In human post-mortem tissue, high levels of PBR ligand-binding were seen in intact glioma cells, while necrotic areas of the tumor and cells in surrounding normal tissue did not display detectable levels of PBR ligand-binding [49]. In addition, [^{3}H]PK 11195 binding in specimens of human gliomas suggested that PBR characteristics may be used to differentiate high from low grade gliomas [50]. Treatment with the specific PBR ligands, PK 11195 and Ro 5-4864, can induce morphological changes, both in rat C6 and human T98G glioma cells [51]. Ikezaki and Black [41] showed that for rat C6 glioma cells, growth rate and thymidine incorporation increased by 20–30% after PK 11195 exposure in the nanomolar range.

In the current study, we examined the relationship between PBR expression and cell growth characteristics in three well-characterized brain glioma cell lines (C6 from rat, and U87MG, and T98G from human). In particular, we studied the PBR binding density in these three cell lines together with the relative in vitro tumorigenicity of these cell lines as assessed by their ability to form colonies in soft agar, as a measure of anchorage independent cell growth. In addition, we assayed these glioma cell's proliferation and cell death characteristics in culture. Furthermore, we assayed the effects of PBR ligands apoptosis in these cell lines. This study suggests that PBR levels are positively correlated with glioma cell tumorigenicity.

1. Materials and methods

1.1. Materials

The cell lines C6, U87MG, and T98G were used, as described by the American type culture collection: C6 glial tumor from rat (tissue, glial cell, glioma); U87MG glioma from human (tissue: glioblastoma; astrocytoma); and T98G glioma from human (tissue: *Glioblastoma multiforme*).

Culture medium for C6 and U87MG consisted of Dulbecco modified eagle medium (with glucose 4500 mg/l, without sodium pyruvate and L-glutamine) (DMEM) with addition of a 200 mM L-glutamine saline solution (2%, v/v). Culture medium for T98G consisted of minimum essential medium Eagle with non-essential amino acids, Earle's salts base, without L-glutamine (MEM) with addition of a solution of 100 mM sodium pyruvate solution (1%, v/v). In all cases, fetal calf serum (10%, v/v), penicillin–streptomycin solution (10 000 units/ml penicillin sodium salt and 10 mg/ml streptomycin sulfate) (1%, v/v), and Amphotericin B-solution (2.5 mg/ml) (0.1%, v/v) was added to the culture media.

Culture medium ingredients were obtained from Biological Industries, Beit HaEmek. [^{3}H]PK 11195 was obtained from New England Nuclear. Unlabeled PK 11195 was purchased from Sigma-Aldrich. The Cell Proliferation Kit (Cell Proliferation Assay with XTT Reagent) was obtained from Biological Industries, Beit HaEmek. The Cell Death Kit (Cell Death Detection ELISA^{PLUS} Kit) was obtained from Roche Molecular Biochemicals. Nylon mesh (30 μm) for cell separation necessary for the FACS analysis was obtained from Sinun, Petach Tikvah. All other compounds were purchased from commercial sources.

1.2. PBR binding

[^{3}H]PK 11195 binding results were assessed in cells that were super-confluent. To collect the cells for the binding assay, the cells were scraped from the flasks in their culture medium. The cells were centrifuged (1000 × *g*, 10 min), resuspended in 1 ml of medium and centrifuged (1000 × *g*, 10 min). The pellet was snap-frozen in liquid nitrogen and stored at −70 °C until further use. For further processing, the pellet was thawed and homogenized in 3 ml of PBS using a Kinematika Polytron (setting 6) for 10 s and centrifuged at 37 000 × *g* for 30 min. The pellet was resuspended in 1 ml of PBS, and homogenized and centrifuged as just described. The pellet was resuspended in 1 ml of PBS. Protein content was determined by the method of Bradford [52] using BSA as a standard. Binding of [^{3}H]PK 11195 to membranes of the various cell lines were conducted as previously described [16,24,32,53]. The reaction mixture contained 400 μl of the homogenized membranes in question (40 μg protein) and 25 μl of [^{3}H]PK 11195 solution (final concentration, 6 nM [specific activity: 85 Ci/mmole]) in the absence (total binding) or presence (non-specific binding) of 75 μl unlabeled PK 11195 (10 μM final concentration). After incubation for 60 min at 4 °C, the samples were vacuum filtered through Whatman GF/C filters, washed three times with 4 ml of 50 mM potassium phosphate buffer (pH 7.4), and placed in vials containing 4 ml of Opti-Fluor. Radioactivity was counted after 12 h with a 1600 CA Tri-Carb liquid scintillation analyzer (Packard).

In addition, saturation curves were determined with Scatchard analysis in the C6 and T98G cell lines, using six concentrations from 0.2 to 6 nM [^{3}H]PK 11195) as described previously [18,24,32,53].

1.3. Cell growth in soft agar

This assay was done according to previously described methods [54,55]. Briefly, for each cell line, bacto-agar was used to prepare, a solution of 0.6% agar in culture medium. To each 25 cm^2 plate, 6 ml of the 0.6% agar solution was added and allowed to solidify for 24 h at room temperature. A 0.3% agar solution was prepared by mixing half of one part of 2×concentrated medium, one-quarter part of sterile double-distilled water, 3×10^4 cells per cell line, and one-quarter part of a 1.2% agar solution warmed to 48 °C. Of this mixture, 1.5 ml was added on top of the agar in the prepared wells. In these wells, the cells were allowed to proliferate for 21 days. To assay anchorage independent cell growth, colony sizes were analysed with a Zeiss Axioscop 2 inverted microscope and Image ProPlus® software version 4.5.1.25 for Windows was used. Briefly, the wells were subdivided in 16 approximately equal-sized areas and from the centers of five such subdivisions, the square measures of the observed colonies were determined. In addition, from four of such locations cell numbers per cell colony were determined.

1.4. Cell proliferation and cell death assays

Cell counts were performed as described previously [24,32]. Briefly, to determine the proliferation rate and the percentage of cell death, 4×10^5 cells were seeded in 25 cm^2 flasks for each cell line and allowed to proliferate for 72 h. Then the medium covering the cells was collected, the cells were trypsinized and added to the collected medium, and a sample was taken for cell counting. The cells were counted visually using an inverted microscope (Olympus CK2), with the aid of a hemocytometer. To determine the percentage of dead cells, cells were stained with Trypan blue at a final concentration of 0.25%.

1.5. XTT cell proliferation analysis

Cells of each cell line were seeded in a 96-well plate (1.5×10^3 cells per well) and allowed to proliferate for 72 h. XTT reagent solution was prepared according to the manufacturer's instructions. To each well, pre-seeded with cells, 50 μl of the XTT reagent solution was added, mixed by gentle agitation, and incubated for 2 h at 37 °C. Absorbance of the samples was measured with an ELISA reader at a wavelength of 450 nm. Reference absorbance (to measure non-specific readings) was measured using a 690 nm wavelength.

1.6. Apoptosis

To determine differences in apoptosis between C6, U87MG, and T98G, we used the Cell Death Kit. For this assay of programmed cell death, 4×10^5 cells were seeded and counted as described in Section 1.4. A fraction of the suspension containing 10^6 cells was centrifuged (1000 × *g*, 5 min), the pellet was resuspended in 1 ml medium, centrifuged (1000 × *g*, 5 min), and the pellets were snap frozen in liquid nitrogen and stored at −70 °C until use. For apoptosis assay, the pellets were allowed to thaw, and then resuspended with lysis buffer according to the manufacturer's instructions. The lysate was centrifuged at 200 × *g* for 10 min. A fraction of the supernatant was transferred to streptavidin-coated microtiter plate modules. Immunoreagent was added (anti-histone-biotin and anti-DNA-peroxidase in incubation buffer), and after incubation with gentle shaking for 2 h, the modules were rinsed three times with incubation buffer. Then the signal for apoptosis was measured following incubation for 20 min with 2,2′-azino-bis-[3-ethylbenzothiazoline]-6-sulfonic acid (ABTS) solution, according the manufacturer's instructions. The level of staining by the ABTS solution was determined with an ELISA reader. Absorbance of the samples was measured at a wavelength of 405 nm. Reference absorbance (to measure non-specific readings) was

measured using a 490 nm wavelength. The ABTS solution by itself was used as a blank.

1.7. Flow cytometric analysis (FACS) of the pre-G1 phase

Flow cytometric analysis was used to monitor the pre-G1 phase (DNA fragmentation) of the cell cycle profile of C6, U87MG, and T98G to assess their basic levels of apoptosis, according to methods described previously [32,56]. Briefly, 4×10^5 cells were seeded in 25 cm^2 flasks, allowed to proliferate for 72 h. Then the medium covering the cells was collected and the cells were trypsinized and added to the collected medium. The cell suspension was centrifuged ($300 \times g$, 5 min) and the pellet resuspended in 1 ml of PBS twice at 4 °C. Then each cell pellet was resuspended in 400 μl of a 70% ethanol solution and incubated for 1 h at 20 °C. Then 600 μl PBS was added to each suspension and mixed, followed by centrifugation ($1000 \times g$, 5 min) at 4 °C. The pellets were resuspended and incubated in 500 μl PBS containing 100 μg/ml RNAase and 0.5% Triton X-100 for 30 min at 37 °C. Then propidium iodide was added to a final concentration of 100 μg/ml for an incubation of 10 min at 4 °C to stain the cell nuclei. The cells were then filtered through a (30 μm) nylon mesh and vortexed briefly before FACS analysis. The flow cytometer used was the FACScan (Becton Dickinson).

1.8. PBR ligand treatment and apoptosis

To assay, whether PBR ligands affected apoptosis in our paradigm, T98G cells were treated with Ro5-4864 and PK 11195, and C6 cells were treated with Ro5-4864. Briefly, 4×10^5 cells of these cell lines were seeded in 25 cm^2 flasks and allowed to proliferate for 72 h, as described in Section 1.4. In addition, 10^{-5} M Ro5-4864 or PK 11195 was added to the medium in half of the flasks. The other half of the flasks were used as controls. Subsequently, cells were collected and used for apoptosis assays, as described in Section 1.6.

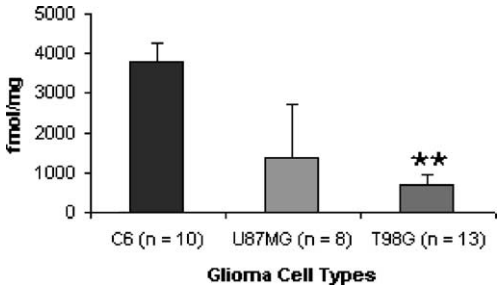

Fig. 2. Differences in [^{3}H]PK 11195 (6 nM) binding between the C6, U87MG, and T98G cell lines expressed in fmol/mg protein. ** C6 vs. T98G: $P < 0.01$.

1.9. Statistical analysis

For statistical analysis, experimental and control groups were usually at $n = 4$. Results are presented as mean ± S.D. In one instance S.E.M. was applied (cell counts of colonies growing in soft agar, Fig. 4B). Non-parametric Kruskal–Wallis and post hoc tests (Dunn's multiple comparison tests) were usually used, since in most cases S.D. differed significantly between groups as indicated by Bartlett's test for homogeneity of variance. In the case of cell counts of

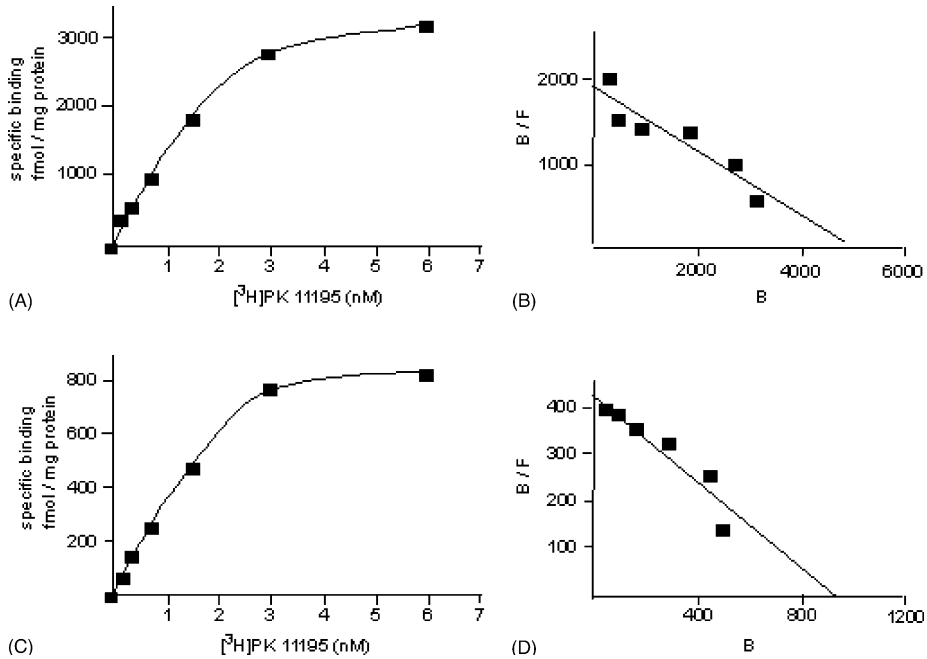

Fig. 3. To the left, representative examples of saturation curves of [^{3}H]PK 11195 binding to membranes of C6 (A) and T98G (C) cells. To the right, Scatchard plots of the saturation curves of [^{3}H]PK 11195-specific binding to membranes of C6 (B) and T98G (D) cells. B : bound; B/F : bound/free.

colonies in soft agar, parametric ANOVA with Student–Newman-Keuls post hoc tests were used, since S.D. did not differ significantly. The significance of the effects of the PBR ligands on apoptosis was determined by the Mann–Whitney tests. $P < 0.05$ was considered statistically significant [57].

2. Results

2.1. PBR binding levels and in vitro tumorigenicity

We found that PBR binding levels (Figs. 2 and 3) and in vitro tumorigenicity (Figs. 4 and 5) appeared to correlate positively with the three cell lines (C6, U87MG, and T98G) studied. C6 showed the highest PBR-binding density of the three cell lines, T98G the lowest, and U87MG showed intermediate levels. In particular, the difference between C6 and T98G was statistically very significant ($P < 0.01$; Fig. 2). The binding is saturable as can been seen in Fig. 3. As a measure of in vitro tumorigenicity, we used the ability of C6, U87MG, and T98G cells to establish anchorage independent growth in soft agar (Figs. 4 and 5). C6 displayed the largest average size of cell colonies, indicative of anchorage independent growth, T98G the smallest, and the sizes of the U87MG colonies were in between those of C6 and T98G (Figs. 4 and 5A). The statistical differences in average colony sizes were highly significant ($P < 0.001$) between all cell lines. With an additional assay, counting cells per colony (Fig. 5B), it was also found that especially C6 displayed the greatest number of large colonies (>400 cells per colony) and medium sized colonies (100–400 cells per colony), while T98G was not able to grow colonies greater than 100 cells per colony. C6 also displayed the lowest number of small colonies (<100 cells per colony). The numbers of cells per colony of U87MG cells were in between those of C6 and T98G, for small, medium, and large colonies.

Taken together, the relatively high C6 PBR-binding levels appear to be associated with larger colonies, while the relatively low T98G PBR binding levels appear to correlate with the inability of these cells to proliferate effectively in soft agar. U87MG appears to take an intermediate position regarding these two parameters of PBR-binding and ability to grow in soft agar.

2.2. Proliferation rate and cell death, including apoptosis

Increased in vitro tumorigenicity (soft agar assay) could be due to higher proliferation rate and/or decrease in death rate. In order to clarify these possibilities, we evaluated C6, U87MG, and T98G proliferation and cell death rates. Proliferation rate, was assayed by visually counting cells with the aid of a hemocytometer (Fig. 6A), as well as, by using the XTT assay of the Cell Proliferation Kit (Fig. 6B).

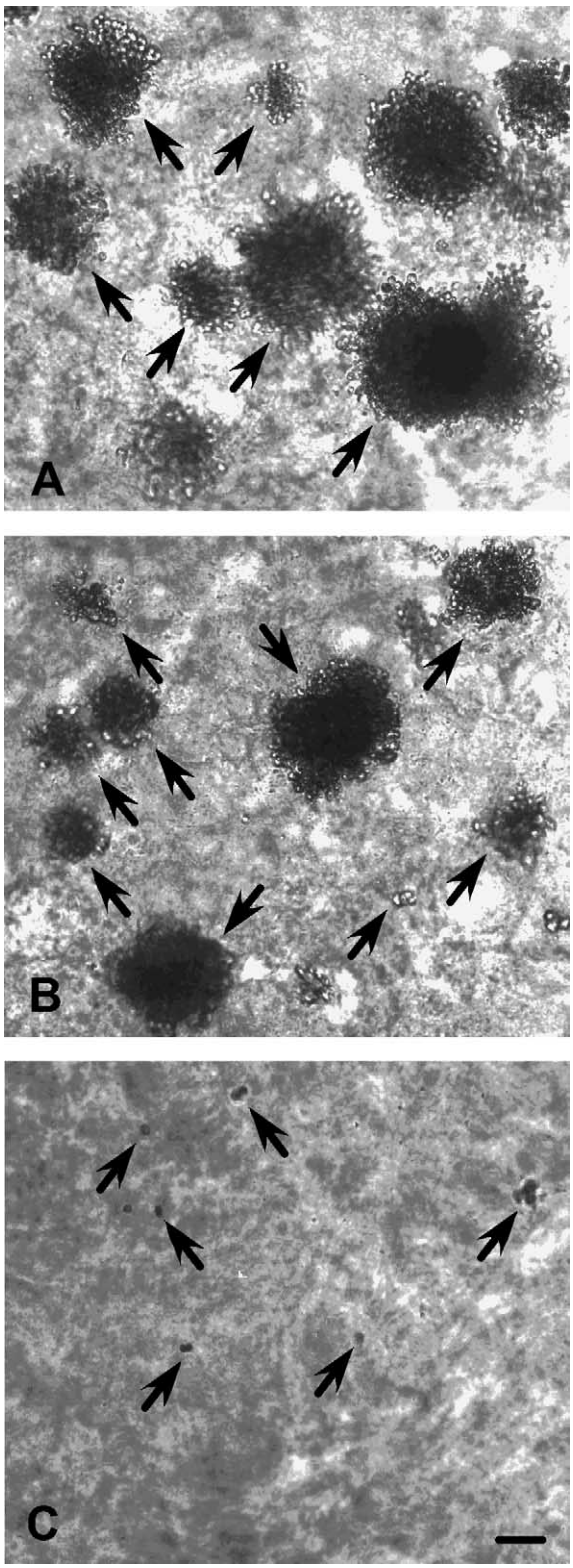

Fig. 4. Micrographs of C6, U87MG, and T98G cells growing in soft agar indicating their in vitro tumorigenicity. (A) C6; (B) U87MG; and (C) T98G. The arrows point at the colonies. The scale bar is 100 μm.

The highest proliferation rate was shown for C6, the lowest for T98G, and intermediate for U87MG (Fig. 6A and B). In particular, the differences in cell proliferation rate between C6 and T98G measured with the two different methods

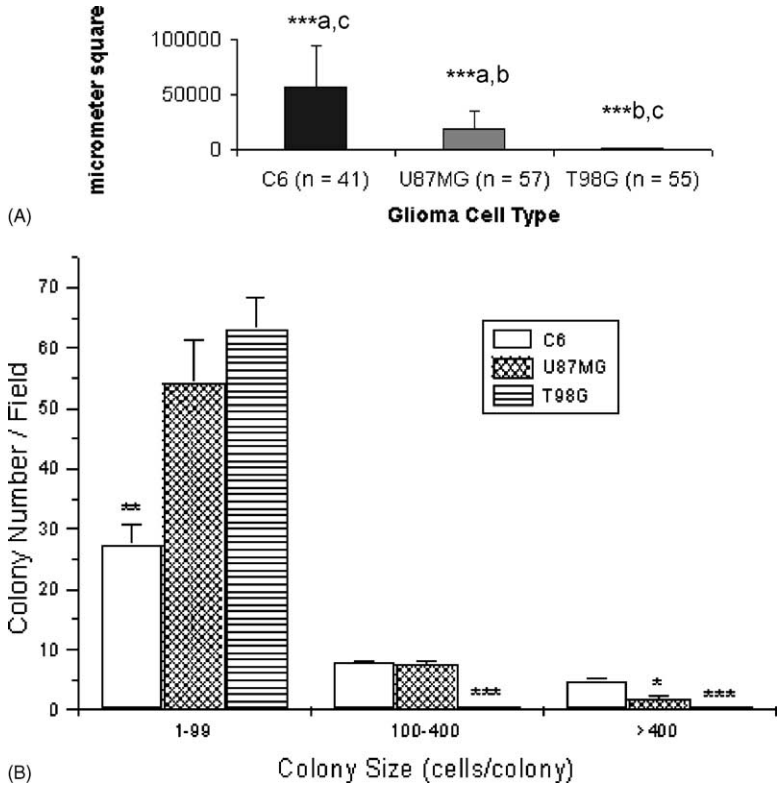

Fig. 5. Anchorage independent cell growth as derived from colonies sizes in soft agar as an indication of tumorigenicity. (A) differences in average colony size of C6, U87MG, and T98G cells growing in soft agar indicating their in vitro tumorigenicity: C6 vs. U87MG, $P < 0.001$ (***a); U87MG vs. T98G, $P < 0.001$ (***b); C6 vs. T98G, $P < 0.001$ (***c). (B) differences in cell number per colony of C6, U87MG, and T98G cells growing in soft agar as a measure of in vitro tumorigenicity (colony size 1–99, C6 very significantly different from U87MG and T98G, $^{**}P < 0.01$; colony size 100–400, C6 highly significantly different from T98G, $^{***}P < 0.001$; and colony size >400, C6 significantly different from U87MG, $^{*}P < 0.05$, and highly significantly different from T98G, $^{***}P < 0.001$).

were highly significant ($P < 0.001$). In addition, the XTT assay also suggested that differences in proliferation rates between C6 and U87MG were also very significant ($P < 0.01$). Similarly, with the XTT assay, differences between U87MG and T98G proliferation rates also appeared to be significant ($P < 0.05$). Thus, both the cell count and the XTT assay suggests that the proliferation rate of T98G is substantially less than of C6, while U87MG displays an intermediate proliferation rate. Thus, the relatively large colonies of C6 in soft agar appear to correlate with a relatively high proliferation rate, while the inability of T98G to grow medium to large colonies appears to correlate with a relatively low proliferation rate. U87MG appears to take an intermediate position regarding these two parameters of colony size and proliferation rate.

Cell death assessed by counting Trypan blue stained C6, U87MG and T98G cells, showed the lowest percentage of cell death in C6, the highest percentage in T98G, and intermediate values in U87MG (Fig. 6C). The six-fold difference in the percentage of cell death between C6 and T98G was highly significant ($P < 0.001$). Apoptosis as measured by the Cell Death Kit, which is a measure of DNA fragmentation, showed the lowest basal levels for C6 cells, the highest levels for T98G cells, and intermediate levels for U87MG cells (Fig. 6D). In particular, the measured difference in apoptosis between C6 and T98G was significant ($P < 0.05$). Thus, both cell death as determined with Trypan blue staining and apoptosis as determined using the Cell Death Kit showed the lowest levels in C6, which also displayed the largest colonies in soft agar. T98G, which showed the smallest colonies in soft agar, showed the highest levels of cell death and apoptosis. U87MG showed intermediate levels for these parameters.

2.3. Cell cycle analysis

Another approach to assess apoptosis is measuring changes in the pre-G1 phase (DNA fragmentation) of the cell cycle profile for a particular cell line. Cell cycles profiles as determined by FACS analysis of C6, T98G, and U87MG demonstrated low pre-G1 levels for C6 cells and progressively higher levels for U87MG and T98G, respectively (Fig. 7). In particular, the difference between C6 and T98G was highly significant ($P < 0.001$) for this phase of the cell cycle (Fig. 7), which is consistent with what was found with the apoptosis assays (Fig. 6D) done with the Cell Death Kit. Thus, our various assays of cell proliferation and cell death uniformly indicated that the changes in cell death appear to be inversely proportional to the measurement of cell proliferation (Figs. 6 and 7).

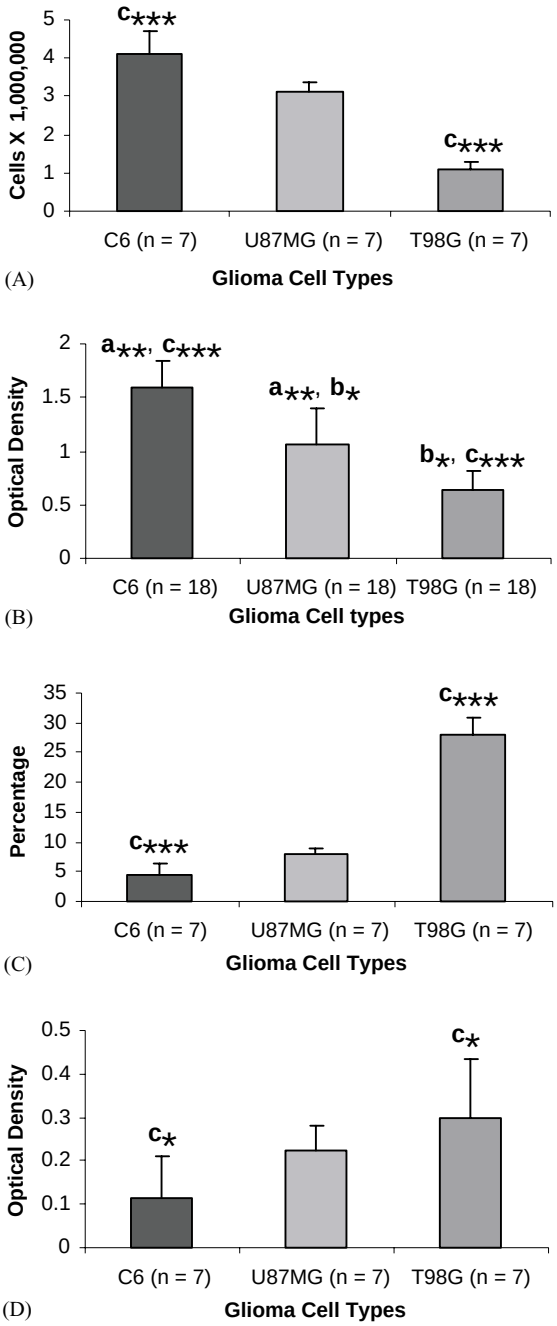

Fig. 6. Differences in proliferation and cell death characteristic between C6, U87MG, and T98G. (A) cell number counted with the aid of a hemocytometer. C6 vs. U87MG (n.s.), U87MG vs. T98G (n.s), C6 vs. T98G ($P < 0.001$, c^{***}); (B) optical density as a measure of relative proliferation determined with the Cell Proliferation Kit. TC6 vs. U87MG ($P < 0.01$, a^{**}), U87MG vs. T98G ($P < 0.05$, b^{*}), C6 vs. T98G ($P < 0.001$, c^{***}); (C) percentage of dead cells among the total number of cells assayed with the aid of Trypan blue staining. C6 vs. U87MG (n.s.), U87MG vs. T98G (n.s.), C6 vs. T98G ($P < 0.001$, c^{***}); and (D) optical density as a measure of apoptosis as determined with the Cell Death Kit. C6 vs. U87MG (n.s.), U87MG vs. T98G (n.s.), C6 vs. T98G ($P < 0.05$, c^{*}).

2.4. PBR ligand treatment and apoptosis

Ro5-4864 treatment of T98G cells reduced basic apoptotic levels by 51% in this cell line (Fig. 8). This effect on apoptosis was highly significant ($P < 0.001$). PK 11195 treatment of T98G cells did not have a significant effect on basic apoptosis in this cell line (not shown). Ro5-4864 treatment of C6 cells reduced basic apoptotic levels by 35% in this cell line (Fig. 8). This effect on apoptosis was significant ($P < 0.05$).

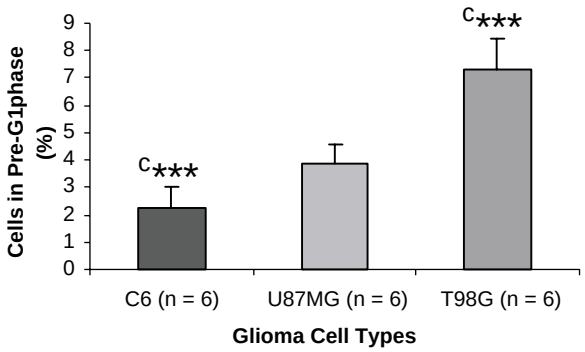

Fig. 7. Differences in percentages of DNA fragmentation determined with flow cytometry as an indication of relative apoptotic levels of C6, U87MG, and T98G. The percentage of T98G cells in the pre-G1 phase is highly significantly higher than of C6 ($P < 0.001$, c^{***}).

3. Discussion

The present study suggests that high levels of PBR expression in glioma cells may correlate positively with tumorigenicity. In particular, C6 glioma cells, which displayed relatively high levels of PBR-binding density, exhibited also potent in vitro tumorigenicity, as determined by its ability to form large colonies in soft agar. In contrast, T98G cells, which displayed relatively low levels of PBR-binding density, were marginally able to proliferate in soft agar, i.e. showed low tumorigenicity. U87MG was intermediate in these respects. Studies on intracranial C6 tumors in rats and U87MG tumors in nude athymic mice also suggested that PBR-density is higher in C6 than in U87MG [58]. While comparative analysis of anchorage independent growth have not been done before on C6, T98G, and U87MG together in one study, separate reports on anchorage independent growth of these three cell lines are in accord with our findings on their relative ability to form colonies in soft agar [59–61]. Potent tumorigenicity, in vitro, as we have described here for C6 cells growing in soft agar, is indicative for tumorigenicity of glial cells, in vivo, as was also found for other systems [62–65]. Thus, our study suggests that in glioma cell lines PBR expression may be predictive for in vivo tumorigenicity. This is in accord with a previous study, suggesting that over-expression of PBR can serve as a prognostic marker for human colorectal cancer [42].

The cell proliferation rate assays (XTT analysis and cell counts) and cell death assays (Trypan blue, and apoptosis assays with the Cell Death Kit and determination of the pre-G1 with FACS analysis), we applied, suggests that C6

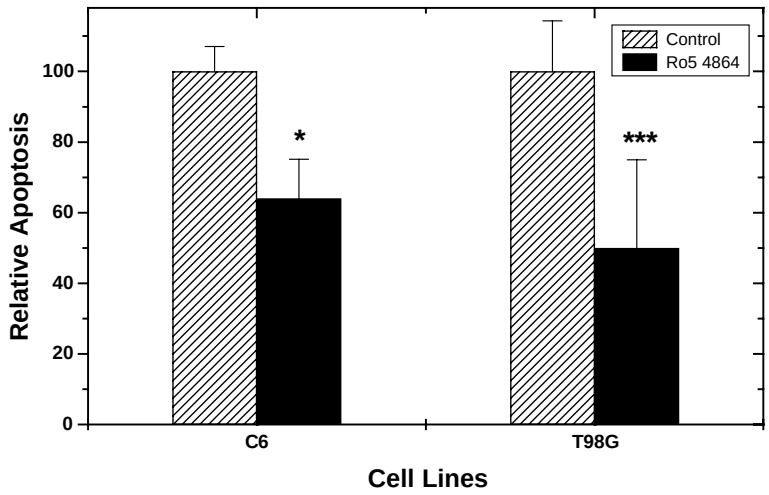

Fig. 8. The effect of 10^{-5} M Ro5-4864 on basic apoptotic rates in C6 and T98G as determined with the Cell Death Kit. Optical density indicative of apoptosis is significantly lower in C6 cells treated with Ro5-4864 as compared to untreated control ($P < 0.01$, *) and highly significantly lower in T98G cells treated with Ro5-4864 as compared to untreated control ($P < 0.001$, ***). Lined boxes are the control cultures, while black boxes represent cultures treated with Ro5-4864.

tumorigenicity is related both to its relatively high proliferation rate and low cell death rate. The opposite is true for T98G. U87MG shows values for these various parameters in ranges intermediate between those of C6 and T98G. Thus, our present study suggests that higher PBR expression, as found in C6, may be associated with both greater cell proliferation rates and lower levels of cell death in glioma cells potentially leading to enhanced tumorigenicity.

While our apoptosis assays show that apoptotic levels for unchallenged C6 cells are low, it was found previously that cadmium can relatively easily induce apoptosis in C6 cell compared to E367 neuroblastoma cells and NIH3T3 fibroblasts [64]. This apoptotic process appears to involve a breakdown of the mitochondrial membrane potential and the activation of caspase 9, suggesting that the PBR complex may be involved in this type of apoptosis. In addition, previous studies have shown that PBR contribute to the maintenance of the mitochondrial potential [43,65,66]. In addition, other studies have shown that the PBR ligand FGIN-1-27 is able to induce apoptosis in colorectal cancer cells [43]. Our study, using glioma cells, indicated that the PBR ligand Ro5-4864 is able to reduce basic apoptotic levels in these cell lines (Fig. 8), while PK 11195 did not have an effect on apoptosis in this paradigm. Other studies also suggested anti-apoptotic effects of PBR ligands [67,68]. As of now, the reason of the discrepancies between the various studies is not clear. They may depend on cell type, growing stage of the cells used, type and/or concentration of the PBR ligands used, etc. Nonetheless, our present study as well as other studies applying PBR ligands suggest that PBR indeed are relevant for apoptosis.

Regarding proliferation, it was found that PK 11195 and Ro5-4864 in the nanomolar range increased the proliferation rate of C6 glioma cells by 20–30% [41]. In the micromolar range, however, these ligands inhibited proliferation [41]. Interestingly, treatment with PK 11195 and Ro5-4864 in the nanomolar range caused a shift of mitochondria from the peripheral cytoplasm to the perinuclear region in C6 cells [51]. It was suggested that this translocation was related to nuclear activity, such as mitotic activity [51]. These data support our notion that in C6 cells PBR may exert a regulatory role on proliferation rate. In addition, it was found that C6 and T98G mitochondria respond differently to PK 11195 or Ro5-4864 treatment [51]. For example, in C6, the number and area of mitochondria per 100 μm^2 increased 250 and 330%, respectively, while in T98G no such effects were discerned [51]. It may be, due to the higher density of PBR in C6, that mitochondria in C6 show a stronger response to PBR ligands than mitochondria in T98G. Interestingly, specific PBR ligands (10–100 μM) induce an arrest in the G_1/G_0 phase of the cell cycle in human breast cancer and colorectal cancer cells [43], suggesting that PBR indeed may be associated with the regulation of the cell cycle and thereby are involved in modulation of cell proliferation.

Thus, it seems that high levels of PBR such as occurrences in C6 cells may be predictive for malignancy, possibly due to enhanced cell proliferation rate and decreased cell death rate. Nonetheless, with the current data it is not possible to detect the exact meaning of PBR-density for tumorigenicity. Presently, we are studying genetically modified PBR over- and under-expressing C6 clones to further clarify whether PBR's role is causative, contributory, or in response to cancer. This may help to design PBR-specific cancer therapies.

Acknowledgments

This research was supported by the U.S.–Israel Binational Science Foundation, Proposal # 9800315: The

relevance of peripheral-type benzodiazepine receptors in brain cancer. The Center for Absorption in Science, Ministry of Immigrant Absorption, State of Israel, is acknowledged for their support to S.L., and L.V.

References

[1] Braestrup C, Squires RF. Specific benzodiazepine receptors in rat brain characterized by high-affinity [^{3}H]diazepam binding. Proc Natl Acad Sci USA 1977;74:3805–9.

[2] Verma A, Snyder SH. Peripheral type benzodiazepine receptors. Ann Rev Pharmacol Toxicol 1989;29:307–22.

[3] Syapin PJ, Skolnick P. Characterization of benzodiazepine binding sites in cultured cells of neural origin. J Neurochem 1979;32:1047–51.

[4] Schoemaker H, Boles RG, Horst WD, Yamamura HI. Specific high-affinity binding sites for [^{3}H]Ro 5-4864 in rat brain and kidney. J Pharmacol Exp Ther 1983;225:61–9.

[5] Itzhak Y, Roig-Cantisano A, Norenberg MD. Ontogeny of peripheral-type benzodiazepine receptors in cultured astrocytes and brain from rat. Dev Brain Res 1995;84:62–6.

[6] Anholt RRH, Pedersen PL, De Souza EB, Snyder SH. The peripheral-type benzodiazepine receptor: localization to the mitochondrial outer membrane. J Biol Chem 1986;261:576–83.

[7] Antkiewicz-Michaluk L, Guidotti A, Krueger KE. Molecular characterization and mitochondrial density of a recognition site for peripheral-type benzodiazepine ligands. Mol Pharmacol 1988;34: 272–8.

[8] Antkiewicz-Michaluk L, Mukhin AG, Guidotti A, Krueger KE. Purification and characterization of a protein associated with peripheral-type benzodiazepine binding sites. J Biol Chem 1988;263:17317–21.

[9] Mukherjee S, Das SK. Subcellular distribution of ''peripheral type'' binding sites for [^{3}H]Ro5-4864 in guinea pig lung. Localization to the mitochondrial inner membrane. J Biol Chem 1989;264:16713–8.

[10] McEnery MW, Snowman AM, Trifiletti RR, Snyder SH. Isolation of the mitochondrial benzodiazepine receptor: association with the voltage-dependent anion channel and the adenine nucleotide carrier. Proc Natl Acad Sci USA 1992;89:3170–4.

[11] Benavides J, Malgouris C, Imbault F, Begassat F, Uzan A, Renault C, et al. ''Peripheral-type'' benzodiazepine binding sites in rat adrenals: binding studies with [^{3}H]PK 11195 and autoradiographic localization. Arch Int Pharmacodyn Ther 1983;266:38–49.

[12] Benavides J, Quarteronet D, Imbault F, Malgouris C, Uzan A, Renault C, et al. Labelling of ''peripheral-type'' benzodiazepine binding sites in the rat brain by using [^{3}H]PK 11195, an isoquinoline carboxamide derivative: kinetic studies and autoradiographic localization. J Neurochem 1983;41:1744–50.

[13] Romeo E, Auta J, Kozikowski AP, Ma D, Papadopoulos V, Puia G, et al. 2-Aryl-3-indoleacetamides (FGIN-1): a new class of potent and specific ligands for the mitochondrial DBI receptor (MDR). J Pharmacol Exp Ther 1992;262:971–8.

[14] Papadopoulos V, Boujrad N, Ikonomovic MD, Ferrara P, Vidic B. Topography of the Leydig cell mitochondrial peripheral-type benzodiazepine receptor. Mol Cell Endocrinol 1994;104:R5–9.

[15] Golani I, Weizman A, Leschiner S, Spanier I, Eckstein N, Limor R, et al. Hormonal regulation of peripheral benzodiazepine receptor-binding properties is mediated by subunit interaction. Biochemistry 2001;40:10213–22.

[16] Veenman L, Leschiner S, Spanier I, Weisinger G, Weizman A, Gavish M. PK11195 attenuates kainic acid-induced seizures and alterations in peripheral-type benzodiazepine receptor (PBR) components in the rat brain. J Neurochem 2002;80:917–27.

[17] Papadopoulos V, Dharmarajan AM, Li H, Culty M, Lemay M, Sridaran R. Mitochondrial peripheral-type benzodiazepine receptor expression. Correlation with gonadotropin-releasing hormone (GnRH) agonist-induced apoptosis in the corpus luteum. Biochem Pharmacol 1999;58:1389–93.

[18] Tsujimoto Y, Shimizu S. VDAC regulation by the Bcl-2 family of proteins. Cell Death Differ 2000;7:1174–81.

[19] Dolder M, Wendt S, Wallimann T. Mitochondrial creatine kinase in contact sites: interaction with porin and adenine nucleotide translocase, role in permeability transition and sensitivity to oxidative damage. Biol Sign Rec 2001;10:93–111.

[20] Papadopoulos V, Guarneri P, Krueger KE, Guidotti A, Costa E. Pregnenolone biosynthesis in C6 glioma cell mitochondria: regulation by diazepam-binding inhibitor mitochondrial receptor. Proc Natl Acad Sci USA 1992;89:5118–22.

[21] Papadopoulos V, Amri H, Boujrad N, Cascio C, Culty M, Garnier M, et al. Peripheral benzodiazepine receptor in cholesterol transport and steroidogenesis. Steroids 1997;62:21–8.

[22] Weizman R, Dagan E, Snyder SH, Gavish M. Impact of pregnancy and lactation on $GABA_A$ receptor and central-type and peripheral-type benzodiazepine receptors. Brain Res 1997;752:307–14.

[23] Weizman R, Leschiner S, Schlegel W, Gavish M. Peripheral-type benzodiazepine receptor ligands and serum steroid hormones. Brain Res 1997;772:203–8.

[24] Kelly-Hershkovitz E, Weizman R, Spanier I, Leschiner S, Lahav M, Weisinger G, et al. Effects of peripheral-type benzodiazepine receptor antisense knockout on MA-10 Leydig cell proliferation and steroidogenesis. J Biol Chem 1998;273:5478–83.

[25] Hirsch JD, Beyer CF, Malkowitz L, Beer B, Blume AJ. Mitochondrial benzodiazepine receptors mediate inhibition of mitochondrial respiratory control. Mol Pharmacol 1989;35:157–63.

[26] Zisterer DM, Gorman AM, Williams DC, Murphy MP. The effects of the peripheral-type benzodiazepine acceptor ligands, Ro 5-4864 and PK 11195, on mitochondrial respiration. Meth Find Exp Clin Pharmacol 1992;14:85–90.

[27] Krueger KE. Molecular and functional properties of mitochondrial benzodiazepine receptors. Biochim Biophys Acta 1995;1241: 453–70.

[28] Ruff MR, Pert CB, Weber RJ, Wahl LM, Wahl SM, Paul SM. Benzodiazepine receptor-mediated chemotaxis of human monocytes. Science 1985;229:1281–3.

[29] Bessler H, Caspi B, Gavish M, Rehavi M, Hart J, Weizman R. Peripheral-type benzodiazepine receptor ligands modulate human natural killer cell activity. Int J Immunopharmacol 1997;19:249–54.

[30] Wang JKT, Morgan JI, Spector S. Benzodiazepines that bind at peripheral sites inhibit cell proliferation. Proc Natl Acad Sci USA 1984;81:753–6.

[31] Nordenberg J, Fenig E, Landau M, Weizman R, Weizman A. Effects of psychotropic drugs on cell proliferation and differentiation. Biochem Pharmacol 1999;58:1229–36.

[32] Carmel I, Fares FA, Leschiner S, Scherubl H, Weisinger G, Gavish M. Peripheral-type benzodiazepine receptors in the regulation of proliferation of MCF-7 human breast carcinoma cell line. Biochem Pharmacol 1999;58:273–8.

[33] Weizman R, Gavish M. Molecular cellular and behavioral aspects of peripheral-type benzodiazepine receptors. Clin Neuropharmacol 1993;16:401–17.

[34] Avital A, Richter-Levin G, Leschiner S, Spanier I, Veenman L, Weizman A, et al. Acute and repeated swim stress effects on peripheral benzodiazepine receptors in the rat hippocampus, adrenal, and kidney. Neuropsychopharmacology 2001;25:669–78.

[35] Torres SR, Frode TS, Nardi GM, Vita N, Reeb R, Ferrara P, et al. Anti-inflammatory effects of peripheral benzodiazepine receptor ligands in two mouse models of inflammation. Eur J Pharmacol 2000;408:199–211.

[36] Miyazawa N, Diksic M, Yamamoto Y. Chronological study of peripheral benzodiazepine binding sites in the rat brain stab wounds using [^{3}H]PK-11195 as a marker for gliosis. Acta Neurochir 1995;137:207–16.

[37] Veenman L, Gavish M. Peripheral benzodiazepine receptors: their implication in brain disease. Drug Dev Res 2000;50:355–70.
[38] Pubill D, Verdaguer E, Canudas AM, Sureda FX, Escubedo E, Camarasa J, et al. Orphenadrine prevents 3-nitropropionic acid-induced neurotoxicity in vitro and in vivo. Br J Pharmacol 2001; 132:693–702.
[39] Gavish M, Bachman I, Shoukrun R, Katz Y, Veenman L, Weisinger G, et al. Enigma of the peripheral benzodiazepine receptor. Pharmacol Rev 1999;51:629–50.
[40] Richfield EK, Ciliax BJ, Starosta-Rubinstein SR, McKeever PE, Penney JB, Young AB. Comparison of [^{14}C]-deoxyglucose metabolism and peripheral benzodiazepine receptor-binding in rat C_6 glioma. Neurology 1988;38:1255–62.
[41] Ikezaki K, Black KL. Stimulation of cell growth and DNA synthesis by peripheral benzodiazepine. Cancer Lett 1990;49:115–20.
[42] Maaser K, Grabowski P, Sutter AP, Hopfner M, Foss HD, Stein H, et al. Overexpression of the peripheral benzodiazepine receptor is a relevant prognostic factor in stage III colorectal cancer. Clin Cancer Res 2002;8:3205–9.
[43] Maaser K, Hopfner M, Jansen A, Weisinger G, Gavish M, Kozikowski AP, et al. Specific ligands of the peripheral benzodiazepine receptor induce apoptosis and cell cycle arrest in human colorectal cancer cells. Br J Cancer 2001;85:1771–80.
[44] Ferrarese C, Appollonio I, Frigo M, Gaini S M, Piolti R, Frattola L. Benzodiazepine receptors and diazepam-binding inhibitor in human cerebral tumors. Ann Neurol 1989;26:564–8.
[45] Black KL, Ikezaki K, Santori E, Becker DP, Vinters HV. Specific high-affinity binding of peripheral benzodiazepine receptor ligands to brain tumors in rat and man. Cancer 1990;65:93–7.
[46] Ikezaki K, Black KL, Santori EM, Smith ML, Becker DP, Payne BA, et al. Three-dimensional comparison of peripheral benzodiazepine binding and histological findings in rat brain tumor. Neurosurgery 1990;27:78–82.
[47] Marcian E, Van Dort ME, Ciliax BJ, Gildersleeve DL, Sherman PS, Rosenspire KC, et al. Radioiodinated benzodiazepines: agents for mapping glial tumors. J Med Chem 1988;31:2081–6.
[48] Takada A, Mitsuka S, Diksic M, Yamamoto YL. Autoradiographic study of peripheral benzodiazepine receptors in animal brain tumor models and human gliomas. Eur J Pharmacol 1992;228:131–9.
[49] Olson JM, Junck L, Young AB, Penney JB, Mancini WR. Isoquinoline and peripheral-type benzodiazepine binding in gliomas: implications for diagnostic imaging. Cancer Res 1988;48:5837–41.
[50] Miyazawa N, Hamel E, Diksic M. Assessment of the peripheral benzodiazepine receptors in human gliomas by two methods. J Neurooncol 1998;38:19–26.
[51] Shiraishi T, Black KL, Ikezaki K, Becker DP. Peripheral benzodiazepine induces morphological changes and proliferation of mitochondria in glioma cells. J Neurosci Res 1991;30:463–74.
[52] Bradford MM. A rapid and sensitive method for the quantitation of microgram quantities of protein utilizing the principle of protein–dye binding. Anal Biochem 1976;72:248–54.
[53] Awad M, Gavish M. Binding of [^{3}H]Ro 5-4864 and [^{3}H]PK 11195 to cerebral cortex and peripheral tissues of various species: species differences and heterogeneity in peripheral benzodiazepine binding sites. J Neurochem 1987;49:1407–14.
[54] Weisinger G, Sachs L. DNA-binding protein that induces cell differentiation. EMBO J 1983;2:2103–7.
[55] Koike M, Elspner E, Campbell MJ, Asou H, Uskokvic M, Tfurvoka N, et al. 19-Norhexafluoride analogues of vitamin D3: a novel class of potent inhibitors of proliferation of human breast cancer cell lines. Cancer Res 1997;57:4545–50.
[56] Vindelov LL, Christensen IJ, Nissen NI. A detergent-trypsin method for the preparation of nuclei for flow cytometric DNA analysis. Cytometry 1983;3:323–7.
[57] Zar JM. Biostatistical analysis. Englewood Cliffs, NJ: Prentice-Hall; 1974. p. 101–62.
[58] Starosta-Rubinstein SR, Ciliax BJ, Penney JB, McKeever PE. Young AB Imaging of a glioma using peripheral benzodiazepine receptor ligands. Proc Natl Acad Sci USA 1987;84:891–5.
[59] Shirsat NV, Shaikh SA. Over-expression of the immediate early gene fra-1 inhibits proliferation, induces apoptosis, and reduces tumourigenicity of C6 glioma cells. Exp Cell Res 2003;291:91–100.
[60] Higashi H, Suzuki-Takahashi I, Yoshida E, Nishimura S, Kitagawa M. Expression of p16INK4a suppresses the unbounded and anchorage-independent growth of a glioblastoma cell line that lacks p16INK4a. Biochem Biophys Res Commun 1997;231:743–50.
[61] Katayama H, Hashimoto Y, Kiyokawa E, Nakaya M, Sakamoto A, Machinami R, et al. Epidermal growth factor-dependent dissociation of CrkII proto-oncogene product from the epidermal growth factor receptor in human glioma cells. Jpn J Cancer Res 1999;90:1096–103.
[62] Condon MS, Bosland MC. The role of stromal cells in prostate cancer development and progression. In Vivo 1999;13:61–5.
[63] Ross RA, Biedler JL, Spengler BA. A role for distinct cell types in determining malignancy in human neuroblastoma cell lines and tumors. Cancer Lett 2003;197:35–9.
[64] Watjen W, Cox M, Biagioli M, Beyersmann D. Cadmium-induced apoptosis in C6 glioma cells: mediation by caspase 9-activation. Biometals 2002;150:15–25.
[65] Zorov DB. Mitochondrial damage as a source of diseases and aging: a strategy of how to fight these. Biochim Biophys Acta 1275:10-15.
[66] Fennell DA, Corbo M, Pallaska A, Cotter FE. Bcl-2 resistant mitochondrial toxicity mediated by the isoquinoline carboxamide PK11195 involves de novo generation of reactive oxygen species. Br J Cancer 1996;200184:1397–404.
[67] Strohmeier R, Roller M, Sanger N, Knecht R, Kuhl H. Modulation of tamoxifen-induced apoptosis by peripheral benzodiazepine receptor ligands in breast cancer cells. Biochem Pharmacol 2002;64: 99–107.
[68] Stoebner PE, Carayon P, Casellas P, Portier M, Lavabre-Bertrand T, Cuq P, et al. Transient protection by peripheral benzodiazepine receptors during the early events of ultraviolet light-induced apoptosis. Cell Death Differ 2001;8:747–53.